A HYBRID AGGRESSIVE SPACE MAPPING ALGORITHM FOR EM OPTIMIZATION

M.H. Bakr, J.W. Bandler, N. Georgieva and K. Madsen

SOS-98-34-R

November 1998

A HYBRID AGGRESSIVE SPACE MAPPING ALGORITHM FOR EM OPTIMIZATION

M.H. Bakr, J.W. Bandler, N. Georgieva and K. Madsen

Simulation Optimization Systems Research Laboratory
and Department of Electrical and Computer Engineering
McMaster University, Hamilton, Canada L8S 4K1

Tel 905 628 9671
Fax 905 628 1578
Email j.bandler@ieee.org

Abstract

We present a novel, Hybrid Aggressive Space Mapping (HASM) optimization algorithm. HASM is a hybrid approach exploiting both the Trust Region Aggressive Space Mapping (TRASM) algorithm and direct optimization. It does not assume that the final space-mapped design is the true optimal design and is robust against severe misalignment between the coarse and the fine models. The algorithm is based on a novel lemma that enables smooth switching from the TRASM optimization to direct optimization and vice versa. The new algorithm has been tested on several microwave filters and transformers.

SUMMARY

Introduction

We present a novel optimization algorithm, Hybrid Aggressive Space Mapping (HASM). Space Mapping (SM) optimization [1, 2, 3, 4] assumes that the circuit under consideration can be simulated using two models: a fine model and a coarse model. The fine model is accurate but is computationally intensive, e.g., a full-wave EM simulator. The coarse model is assumed to be fast but not very accurate. SM optimization directs most of the optimization computational effort towards the coarse model while

This work was supported in part by the Natural Sciences and Engineering Research Council of Canada under Grants OGP0007239, STP0201832 and through the Micronet Network of Centres of Excellence. N. Georgieva is supported by an NSERC Postdoctorate fellowship and M.H. Bakr by an Ontario Graduate Scholarship.

J.W. Bandler is also with Bandler Corporation, P.O. Box 8083, Dundas, Ontario, Canada L9H 5E7.

K. Madsen is with the Department of Mathematical Modelling, Technical University of Denmark, DK-2800 Lyngby, Denmark.

maintaining the accuracy of the fine model. The overall computational effort needed is much smaller than that needed for direct optimization.

The parameter extraction step is a crucial procedure in the Aggressive Space Mapping (ASM) technique [4]. In this step a coarse model point whose response matches a given fine model response is obtained. This is essentially an optimization procedure. The nonuniqueness of the extracted parameters may lead to divergence or oscillation of the iterations [2]. To alleviate this problem the TRASM algorithm was introduced [3]. TRASM integrates a trust region methodology [5] with the ASM technique. Also, it utilizes a recursive multi-point parameter extraction in order to improve the uniqueness of the extraction step.

The design obtained by pure SM optimization in most cases is very near optimal. However, the optimality of the final design can not be guaranteed. This is because the final space-mapped response matches the optimal coarse model response which may be different from the optimal fine model response obtained by direct optimization. The new algorithm is designed to overcome this limitation and handle severely misaligned cases.

Aggressive Space Mapping: A Brief Review

We refer to the vectors of "fine" model parameters and "coarse" model parameters as $\boldsymbol{x}_{em}$ and $\boldsymbol{x}_{os}$, respectively. The first step is to obtain the optimal design of the coarse model $\boldsymbol{x}_{os}^{*}$. ASM aims at establishing a mapping $\boldsymbol{P}$ between the two spaces [4]

$$\boldsymbol{x}_{os} = \boldsymbol{P}(\boldsymbol{x}_{em}) \tag{1}$$

such that

$$\left\| \boldsymbol{R}_{em}(\boldsymbol{x}_{em}) - \boldsymbol{R}_{os}(\boldsymbol{x}_{os}) \right\| \leq \varepsilon \tag{2}$$

where $\boldsymbol{R}_{em}$ is the vector of fine model responses, $\boldsymbol{R}_{os}$ is the vector of coarse mode responses and $\| \ \|$ is a suitable norm. We define the error function

$$\boldsymbol{f} = \boldsymbol{P}(\boldsymbol{x}_{em}) - \boldsymbol{x}_{os}^{*} \tag{3}$$

The final fine model design is obtained and the mapping established by solving the nonlinear system

$$\boldsymbol{f}(\boldsymbol{x}_{em}) = \boldsymbol{0} \tag{4}$$

Let $\boldsymbol{x}_{em}^{(i)}$ be the *i*th iterate in the solution of (4). In the ASM technique, the next iterate $\boldsymbol{x}_{em}^{(i+1)}$ is found by a quasi-Newton iteration

$$\boldsymbol{x}_{em}^{(i+1)} = \boldsymbol{x}_{em}^{(i)} + \boldsymbol{h}^{(i)} \tag{5}$$

where $\boldsymbol{h}^{(i)}$ is obtained from

$$\boldsymbol{B}^{(i)}\,\boldsymbol{h}^{(i)} = -\boldsymbol{f}\,(\boldsymbol{x}_{em}^{(i)}) \tag{6}$$

and $\boldsymbol{B}^{(i)}$ is an approximation to the Jacobian of the vector $\boldsymbol{f}$ with respect to $\boldsymbol{x}_{em}$ at the *i*th iteration. The matrix $\boldsymbol{B}$ is updated at each iteration using Broyden's update [6].

Vector $\boldsymbol{f}$ is obtained by evaluating $\boldsymbol{P}(\boldsymbol{x}_{em})$, which is done indirectly through parameter extraction. This optimization process may have more than one minimum, leading to divergence or oscillation of the ASM technique. The TRASM algorithm [3] was designed to overcome this problem. At the *i*th iteration, the residual vector $\boldsymbol{f}^{(i)} = \boldsymbol{P}(\boldsymbol{x}_{em}^{(i)}) - \boldsymbol{x}_{os}^{*}$ defines the difference between the vector of extracted coarse model parameters $\boldsymbol{x}_{os}^{(i)} = \boldsymbol{P}(\boldsymbol{x}_{em}^{(i)})$ and the optimal coarse model design. The mapping is established by driving this residual vector to zero. It follows that the value $\left\|\boldsymbol{f}^{(i)}\right\|$ can serve as a measure of the misalignment between the two spaces in the *i*th iteration. The *i*th TRASM iteration is obtained from

$$(\boldsymbol{B}^{(i)T}\,\boldsymbol{B}^{(i)} + \lambda\,\boldsymbol{I})\,\boldsymbol{h}^{(i)} = -\boldsymbol{B}^{(i)T}\,\boldsymbol{f}^{(i)} \tag{7}$$

where $\boldsymbol{B}^{(i)}$ is an approximation to the Jacobian of the coarse model parameters with respect to the fine model parameters at the *i*th iteration. Parameter λ is selected such that the step obtained satisfies $\left\|\boldsymbol{h}^{(i)}\right\| \le \delta$, where δ is the size of the trust region.

Space Mapping and Direct Optimization

The HASM algorithm exploits the following novel lemma that allows for smooth switching between direct optimization and SM. The proof is omitted here for the sake of brevity.

Lemma Assume that $\boldsymbol{x}_{os}$ corresponds to $\boldsymbol{x}_{em}$ through a parameter extraction process. Then the Jacobian $\boldsymbol{J}_{em}$ of the fine model responses at $\boldsymbol{x}_{em}$ and the Jacobian $\boldsymbol{J}_{os}$ of the coarse model responses at $\boldsymbol{x}_{os}$ are related by

$$\boldsymbol{J}_{em} = \boldsymbol{J}_{os}\boldsymbol{B} \tag{8}$$

where $\boldsymbol{J}_{os}$ is the Jacobian of the coarse model responses at the point $\boldsymbol{x}_{os}$.

Relation (8) shows that by using $\boldsymbol{B}$ and $\boldsymbol{J}_{os}$ we are able to obtain a good estimate of the Jacobian of the fine model responses without any further fine model simulations. It follows that when ASM optimization is not converging we can switch smoothly to direct optimization. The point reached becomes a starting point for direct optimization, with corresponding first-order derivatives calculated by (8).

It follows from (8) that

$$\boldsymbol{B} = \left(\boldsymbol{J}_{os}^{T}\boldsymbol{J}_{os}\right)^{-1}\boldsymbol{J}_{os}^{T}\boldsymbol{J}_{em} \tag{9}$$

Relation (9) assumes that the $\boldsymbol{J}_{os}$ is full rank and $m \geq n$, where n is the number of parameters and m is the number of responses . It is used for switching back from direct optimization to SM optimization.

The HASM Algorithm

The HASM algorithm exploits SM when effective, otherwise it defaults to direct optimization. The objective function of the TRASM algorithm is

$$\left\|\boldsymbol{f}\right\|_2^2 = \left\|\boldsymbol{P}(\boldsymbol{x}_{em}) - \boldsymbol{x}_{os}^{*}\right\|_2^2 \tag{10}$$

while the objective function for direct optimization is

$$\left\|\boldsymbol{g}\right\|_2^2 = \left\|\boldsymbol{R}_{em}(\boldsymbol{x}_{em}) - \boldsymbol{R}_{os}(\boldsymbol{x}_{os}^{*})\right\|_2^2 \tag{11}$$

While the SM objective (10) aims at matching the optimal coarse model parameters with the extracted coarse model parameters in the parameter space, objective function (11) aims at matching the same points mapped through the appropriate responses in the response space. Solving the matching

problem may be easier in one of these two spaces depending on the functional behavior of the coarse and fine models.

The HASM algorithm consists of two phases: the first phase follows the TRASM strategy while the second exploits direct optimization. It utilizes (8) and (9) for switching between phases as dictated by the smoothness of convergence.

The main objective of the HASM algorithm is to minimize (11). In the *i*th iteration we assume the existence of trusted extracted coarse model parameters $\boldsymbol{x}_{os}^{(i)} = \boldsymbol{P}(\boldsymbol{x}_{em}^{(i)})$. The step taken in this iteration is given by (7) where $\boldsymbol{x}_{em}^{(i+1)} = \boldsymbol{x}_{em}^{(i)} + \boldsymbol{h}^{(i)}$. Single-point parameter extraction is then applied at the point $\boldsymbol{x}_{em}^{(i+1)}$ to get $\boldsymbol{f}^{(i+1)} = \boldsymbol{P}(\boldsymbol{x}_{em}^{(i+1)}) - \boldsymbol{x}_{os}^{*}$.

The new point is accepted and the first phase resumes in two different cases. The first case occurs if this point satisfies certain success criteria with respect to the reductions in both objective functions (10) and (11). $\boldsymbol{B}^{(i)}$ is then updated. The second case occurs if this point satisfies the success criterion for the objective function (11) but does not satisfy the success criterion for (10). However, the vector of extracted parameters obtained by multi-point parameter extraction approaches a limit that satisfies the success criterion for (10).

Switching to the second phase takes place in two different cases. The first case is that the success criterion of (11) is not satisfied which means that we have to reject the new point $\boldsymbol{x}_{em}^{(i+1)}$. The Jacobian of the fine model responses at the point $\boldsymbol{x}_{em}^{(i)}$ is then evaluated. This is done by first evaluating the Jacobian of the coarse model responses $\boldsymbol{J}_{os}^{(i)}$ at the previously extracted coarse model point $\boldsymbol{x}_{os}^{(i)} = \boldsymbol{P}(\boldsymbol{x}_{em}^{(i)})$. $\boldsymbol{J}_{em}^{(i)}$ is then approximated using (8). Both $\boldsymbol{x}_{em}^{(i)}$ and $\boldsymbol{J}_{em}^{(i)}$ are then supplied to the second phase.

The second case occurs when the new point $\boldsymbol{x}_{em}^{(i+1)}$ satisfies the success criterion of (11) but does not satisfy the success criterion of (10). In this case the point $\boldsymbol{x}_{em}^{(i+1)}$ is better than the previous point $\boldsymbol{x}_{em}^{(i)}$ and is accepted. As the vector of extracted parameters does not satisfy the success criterion of (10), the vector $\boldsymbol{f}^{(i+1)}$ can not be trusted. In order to trust this vector, recursive multi-point parameter extraction is

applied at the point $\boldsymbol{x}_{em}^{(i+1)}$ until either $\boldsymbol{f}^{(i+1)}$ approaches a limiting value or the number of additional points used for multi-point parameter extraction reaches n. If $\boldsymbol{f}^{(i+1)}$ approaches a limit that does not satisfy the success criterion of (10), $\boldsymbol{B}^{(i+1)}$ is updated, $\boldsymbol{J}_{os}^{(i+1)}$ at the extracted coarse model point $\boldsymbol{x}_{os}^{(i+1)}=\boldsymbol{P}(\boldsymbol{x}_{em}^{(i+1)})$ is evaluated and $\boldsymbol{J}_{em}^{(i+1)}$ is then approximated using (8). Otherwise, $\boldsymbol{J}_{em}^{(i+1)}$ is approximated using the n+1 fine model points used for multi-point parameter extraction. The second phase is then supplied by the point $\boldsymbol{x}_{em}^{(i+1)}$ and the Jacobian estimate $\boldsymbol{J}_{em}^{(i+1)}$, which is either calculated using (8) or through finite differences.

The second phase utilizes the first-order derivatives supplied by SM to carry out a number of successful iterations. By a successful iteration we mean an iteration that satisfies the success criterion of (11). At the end of each successful iteration parameter extraction is applied at the new iterate $\boldsymbol{x}_{em}^{(k)}$ and is used to check whether the success criterion of (10) is satisfied. If it is satisfied $\boldsymbol{J}_{os}^{(k)}$ is evaluated at the point $\boldsymbol{x}_{os}^{(k)}=\boldsymbol{P}(\boldsymbol{x}_{em}^{(k)})$, $\boldsymbol{B}$ is reevaluated using (9) and the algorithm switches back to the first phase. The superscript k is used as an index for the successful iterates of the direct optimization phase. If the success criterion of (10) is not satisfied phase 2 continues. Fig. 1 illustrates the switching between SM optimization and direct optimization. A flow chart of the HASM algorithm is shown in Fig. 2.

The objective function (11) aims at matching the fine model response to the optimal coarse model response but this does not ensure the optimality of the space-mapped solution if the optimal coarse model response is different from the optimal fine model response. This motivates the suggestion that if the second phase has reached a point where no more improvement in the objective function (11) is possible, direct optimization is used to solve the original design problem in the fine model space using a minimax optimizer [7]. The starting point for the minimax problem is the final design obtained by the two phases. This ensures minimax optimality of the design. The current implementation of the HASM algorithm is in MATLAB [8].

Three-Section Waveguide Transformer

We consider the design of a three-section waveguide transformer [9]. The design constraints are

$$vswr \le 1.04 \text{ for } 5.7 \text{ GHz} \le f \le 7.2 \text{ GHz} \quad (12)$$

The designable parameters are the heights of the waveguide sections b_1, b_2 and b_3 and the lengths of waveguide sections L_1, L_2 and L_3. The fine model exploits HP HFSS [10] through HP Empipe3D [11]. The coarse analytical model, optimized first, does not take into account the junction discontinuity effects [9]. See the second column of Table I.

The optimal coarse model design is taken as the initial fine model design (Fig. 3). The HASM algorithm switched to the second phase after two iterations of the TRASM algorithm, which required 4 fine model simulations. The fine model design at the end of the first phase is given in the third column of Table I. The corresponding response is shown in Fig. 4. The second phase carries out only one iteration which required 2 fine model simulations. The fine model design obtained at the end of the second phase is given in the fourth column of Table I. The corresponding fine model response is shown in Fig. 5.

To ensure optimality a minimax optimizer is applied to the original design problem (12), starting from the design obtained at the end of the second phase. The optimal fine mode design is given in the fifth column of Table I. The optimal fine model response is shown in Fig. 6.

Six-Section H-Plane Waveguide Filter

We consider a six-section H-plane waveguide filter [12, 13]. Design specifications are taken as

$$|S_{11}| \le 0.16 \text{ for } 5.4 \text{ GHz} \le f \le 9.0 \text{ GHz} \quad (13)$$

$$|S_{11}| \ge 0.85 \text{ for } f \le 5.2 \text{ GHz and } |S_{11}| \ge 0.5 \text{ for } 9.5 \text{ GHz} \le f \quad (14)$$

A waveguide with a cross-section of 1.372 inches by 0.622 inches (3.485 cm by 1.58 cm) is used. The six sections are separated by seven H-plane septa, which have a finite thickness of 0.02 inches (0.508 mm). The filter is shown in Fig. 7.

The optimizable parameters are the four septa widths W_1, W_2, W_3 and W_4 and the three waveguide-section lengths L_1, L_2 and L_3. The coarse model consists of lumped inductances and dispersive transmission line sections. The coarse model is simulated using OSA90/hope [14]. There are various approaches to calculate the equivalent inductive susceptance corresponding to an H-plane septum. We

utilize a simplified version of a formula due to Marcuvitz [15] in evaluating the inductances. The coarse model is shown in Fig. 8. The fine model exploits HP HFSS [10] through HP Empipe3D [11].

The coarse model is first optimized using the minimax optimizer available in OSA90/hope. The optimal coarse model design is given in the second column of Table II. The optimal coarse model response is taken as the initial fine model design. The fine model response at the starting point is shown in Fig. 9. This figure shows that the design specifications are violated at the initial fine model design. The algorithm required 4 iterations to reach the final space-mapped design. A total of 5 fine model simulations were needed to obtain the final design. The final space-mapped design obtained at the end of the second phase is given in the third column of Table II. The corresponding fine model response is shown in Fig. 10.

To ensure optimality the minimax optimizer is applied to the fine model. The starting point for the minimax optimizer is the final space-mapped design. The optimal fine model design is given in the fourth column of Table II. The optimal fine model response is shown in Fig. 11.

Conclusions

We present a novel, Hybrid Aggressive Space Mapping (HASM) optimization algorithm. This algorithm enables smooth switching from Space Mapping (SM) optimization to direct optimization if SM fails. The direct optimization phase utilizes all the available information accumulated by SM in direct optimization. The algorithm also enables smooth switching from direct optimization to space mapping if SM is converging smoothly. The connection between SM and direct optimization is based on a novel lemma. A number of examples successfully demonstrate the technique.

References

[1] J.W. Bandler, R.M. Biernacki, S.H. Chen, P.A. Grobelny and R.H. Hemmers, "Space mapping technique for electromagnetic optimization," *IEEE Trans. Microwave Theory Tech.,* vol. 42, 1994, pp. 2536-2544.

[2] J.W. Bandler, R.M. Biernacki and S.H. Chen, "Fully automated space mapping optimization of 3D structures," *IEEE MTT-S Int. Microwave Symp. Dig.* (San Francisco, CA), 1996, pp. 753-756.

[3] M.H. Bakr, J.W. Bandler, R.M. Biernacki, S.H. Chen and K. Madsen, "A trust region aggressive space mapping algorithm for EM optimization," *IEEE MTT-S Int. Microwave Symp. Dig.* (Baltimore, MD), 1998, pp. 1759-1762.

[4] J.W. Bandler, R.M. Biernacki, S.H. Chen, R.H. Hemmers and K. Madsen, "Electromagnetic optimization exploiting aggressive space mapping," *IEEE Trans. Microwave Theory Tech.*, vol. 43, 1995, pp. 2874-2882.

[5] J.J. Moré and D.C. Sorenson, "Computing a trust region step," *SIAM J. Sci. Stat. Comp.*, vol. 4, 1983, pp. 553-572.

[6] C.G. Broyden, "A class of methods for solving nonlinear simultaneous equations," *Math. Comp.*, vol. 19, 1965, pp. 577-593.

[7] J.W. Bandler, W. Kellermann and K. Madsen, "A superlinearly convergent minimax algorithm for microwave circuit design," *IEEE Trans. Microwave Theory Tech.*, vol. MTT-33, 1985, pp. 1519-1530.

[8] MATLAB® Version 5.0, The Math. Works, Inc., 24 Prime Park Way, Natick, MA 01760, 1997.

[9] J.W. Bandler, "Computer optimization of inhomogeneous waveguide transformers," *IEEE Trans. Microwave Theory Tech.*, vol. MTT-17, 1969, pp. 563-571.

[10] HP HFSS™ Version 5.2, HP EEsof Division, 1400 Fountaingrove Parkway, Santa Rosa, CA 95403-1799, 1998.

[11] HP Empipe3D™ Version 5.2, HP EEsof Division, 1400 Fountaingrove Parkway, Santa Rosa, CA 95403-1799, 1998.

[12] L. Young and B.M. Schiffman, "A useful high-pass filter design," *Microwave J.*, vol. 6, 1963, pp. 78-80.

[13] G.L. Matthaei, L. Young and E.M. T. Jones, *Microwave Filters, Impedance-Matching Network and Coupling Structures*. New York: McGraw-Hill, First Edition, 1964.

[14] *OSA90/hope*™ Version 4.0, formerly Optimization Systems Associates Inc., P.O. Box 8083, Dundas, ON, Canada, L9H 5E7, 1997, now HP EEsof Division, 1400 Fountaingrove Parkway, Santa Rosa, CA 95403-1799.

[15] N. Marcuvitz, *Waveguide Handbook*. New York: McGraw-Hill, First Edition, 1951, p. 221.

TABLE I
THE OPTIMAL COARSE MODEL DESIGN AND THE DESIGNS OBTAINED DURING DIFFERENT PHASES OF THE HASM ALGORITHM FOR THE THREE-SECTION WAVEGUIDE TRANSFORMER

Parameter	$\boldsymbol{x}_{os}^{*}$	First Phase Design	Second Phase Design	$\boldsymbol{x}_{em}^{*}$
b_1	0.90318	0.90331	0.90114	0.90549
b_2	1.37093	1.36436	1.35687	1.35777
b_3	1.73609	1.73208	1.72470	1.71866
L_1	1.54879	1.46991	1.47203	1.47008
L_2	1.58375	1.56402	1.56521	1.57587
L_3	1.64590	1.79666	1.77744	1.78286

All values are in cm

TABLE II
THE OPTIMAL COARSE MODEL DESIGN, THE FINAL SPACE-MAPPED AND THE OPTIMAL FINE MODEL DESIGNS FOR THE SIX-SECTION H-PLANE WAVEGUIDE FILTER

Parameter	$\boldsymbol{x}_{os}^{*}$	$\overline{\boldsymbol{x}}_{em}$	$\boldsymbol{x}_{em}^{*}$
W_1	0.48583	0.51326	0.51344
W_2	0.43494	0.47379	0.47396
W_3	0.40433	0.45091	0.45100
W_4	0.39796	0.44675	0.44664
L_1	0.65585	0.63701	0.63695
L_2	0.65923	0.63954	0.63977
L_3	0.67666	0.65704	0.65694

All values are in inches

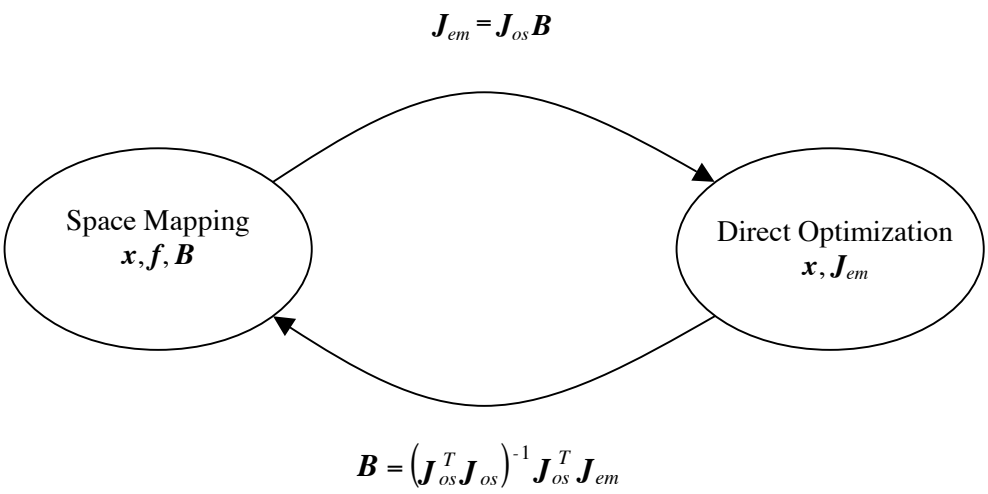

Fig. 1. Illustration of the connection between space mapping and direct optimization.

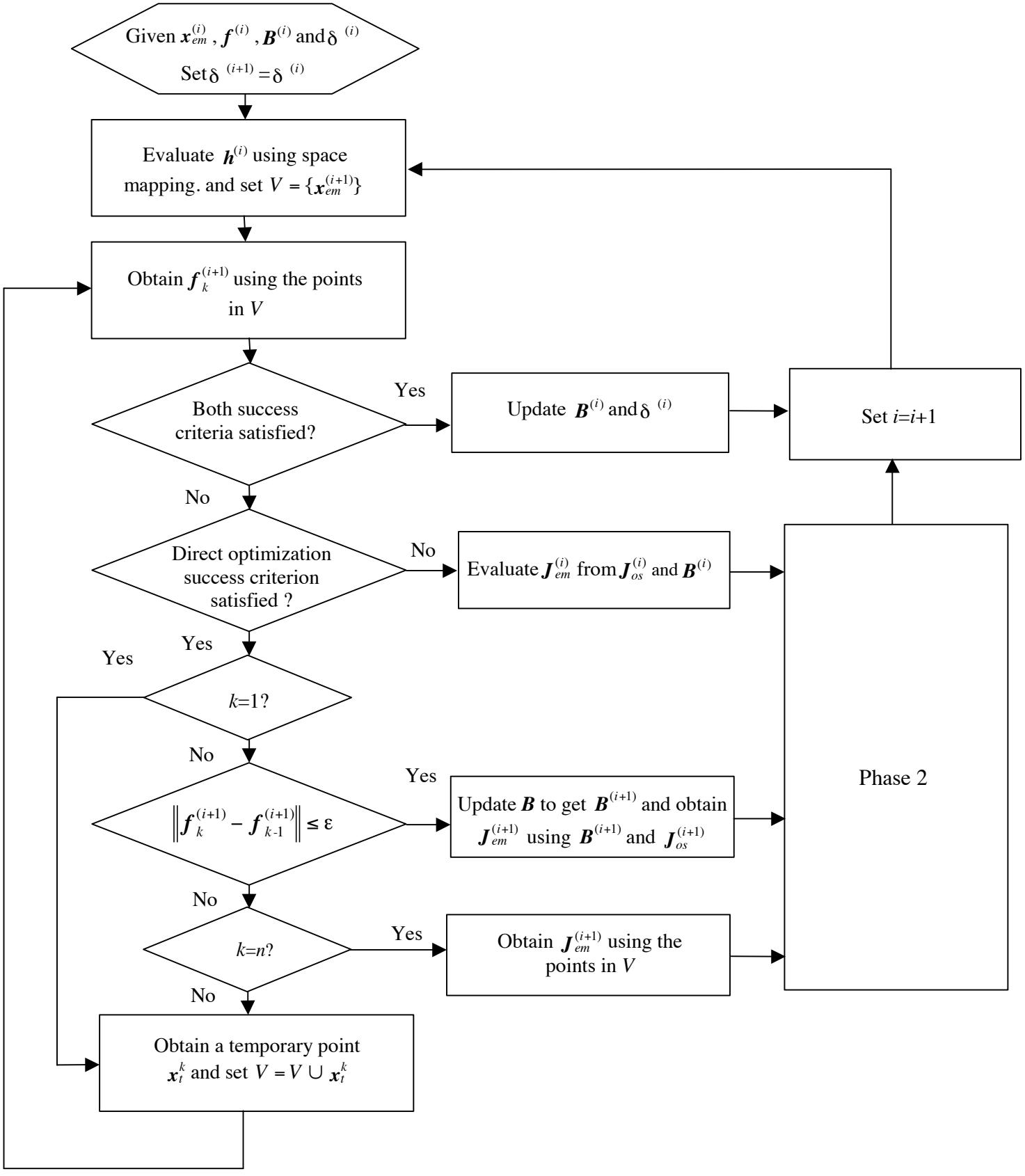

Fig. 2. A flow chart of the first phase of the HASM algorithm.

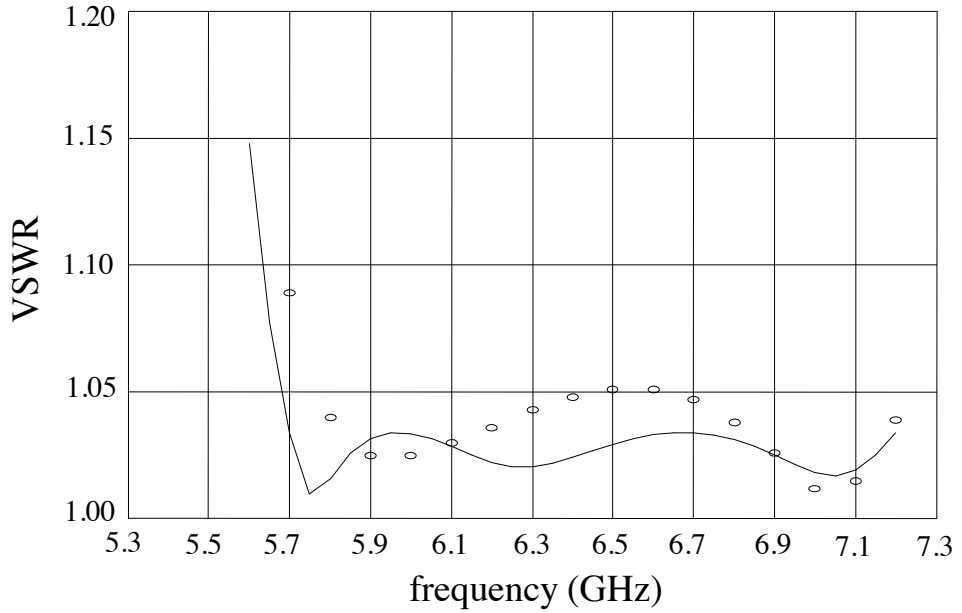

Fig. 3. The optimal coarse model response (—) and the fine model response (o) at the optimal coarse model design for the three-section waveguide transformer.

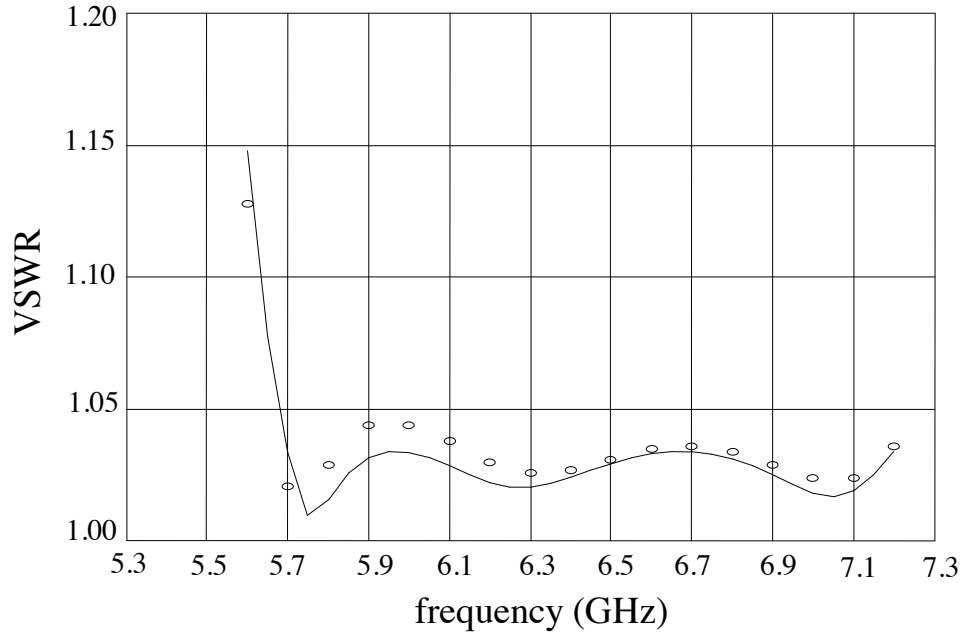

Fig. 4. The optimal coarse model response (—) and the fine model response (o) obtained at the end of the first phase of the HASM algorithm for the three-section waveguide transformer.

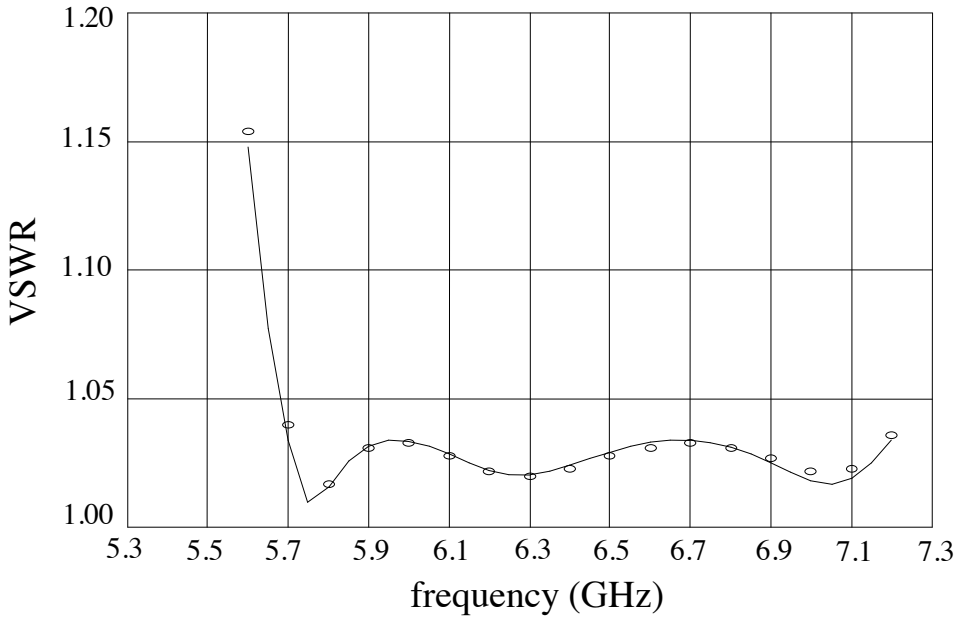

Fig. 5. The optimal coarse model response (—) and the fine model response (o) obtained at the end of the second phase of the HASM algorithm for the three-section waveguide transformer.

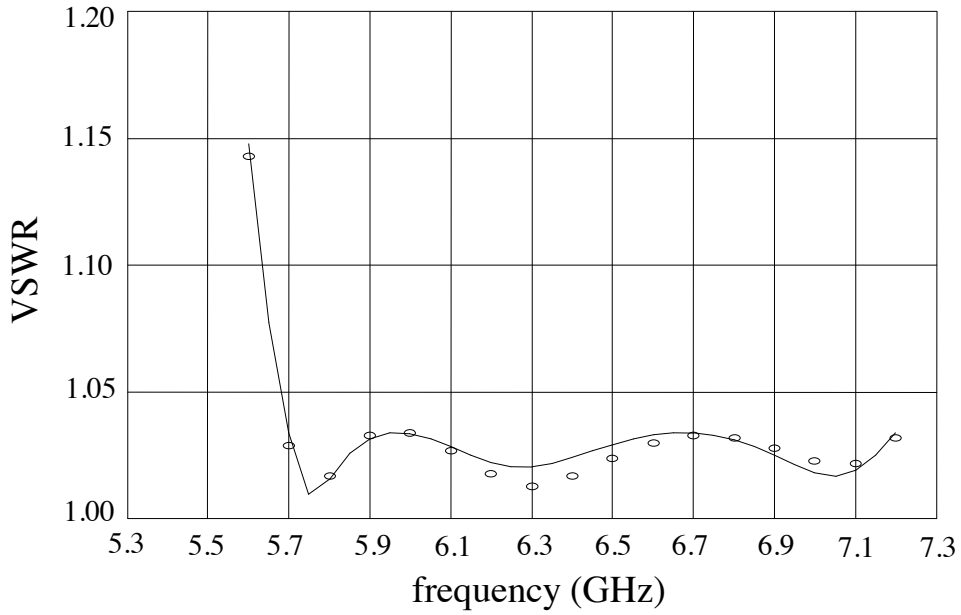

Fig. 6. The optimal coarse model response (—) and the minimax optimal fine model response (o) for the three-section waveguide transformer.

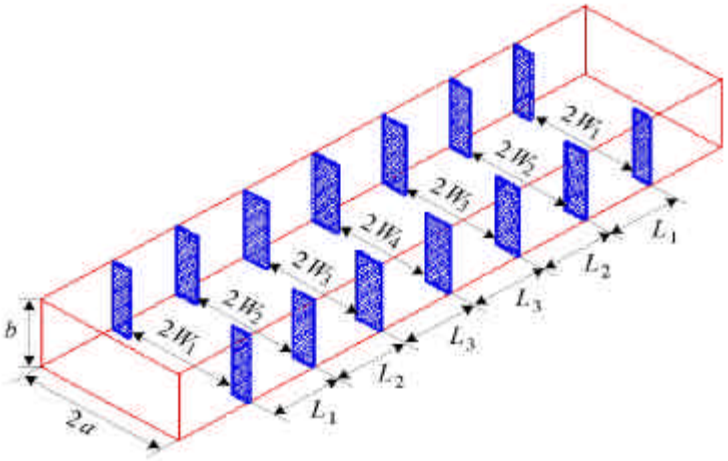

Fig. 7. The fine model of the six-section waveguide filter [12, 13].

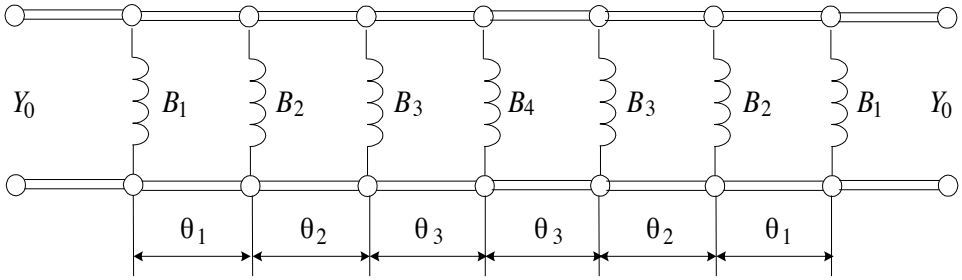

Fig. 8. The coarse model of the six-section waveguide filter [15].

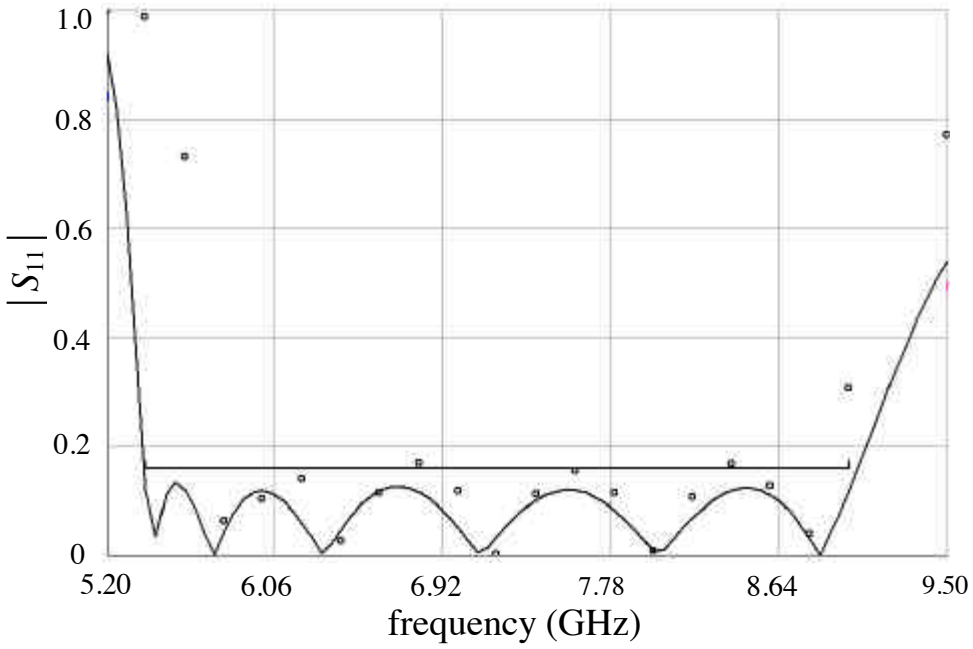

Fig. 9. The optimal coarse model response (—) and the fine model response (o) at the optimal coarse model design for the six-section waveguide filter.

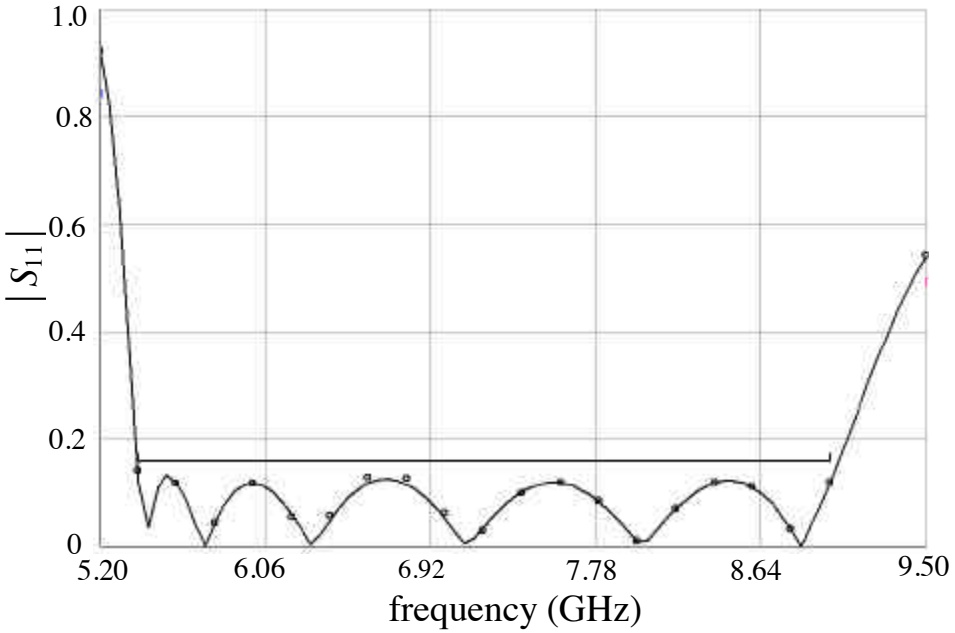

Fig. 10. The optimal coarse model response (—) and the fine model response (o) at the end of the second phase of the HASM algorithm for the six-section waveguide filter.

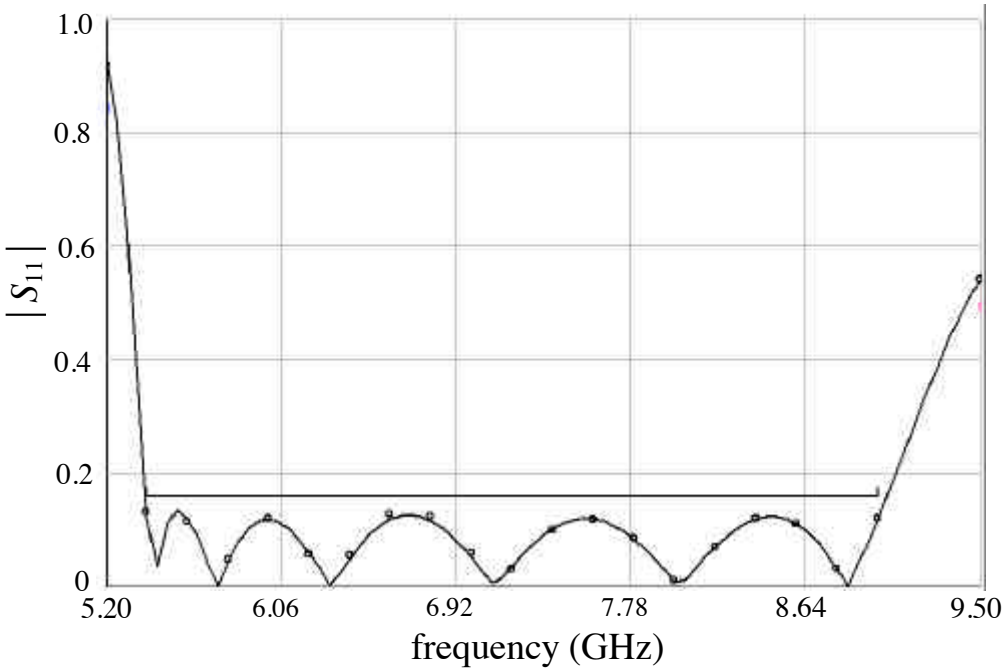

Fig. 11. The optimal coarse model response (—) and the optimal minimax fine model response (o) for the six-section waveguide filter.